

Interaction of firefly luciferase and silver nanoparticles and its impact on enzyme activity

This article has been downloaded from IOPscience. Please scroll down to see the full text article.

2013 Nanotechnology 24 345101

(<http://iopscience.iop.org/0957-4484/24/34/345101>)

View [the table of contents for this issue](#), or go to the [journal homepage](#) for more

Download details:

IP Address: 130.127.189.184

The article was downloaded on 09/08/2013 at 14:10

Please note that [terms and conditions apply](#).

Interaction of firefly luciferase and silver nanoparticles and its impact on enzyme activity

Aleksandr Käkinen^{1,2}, Feng Ding³, Pengyu Chen^{4,5}, Monika Mortimer¹, Anne Kahru¹ and Pu Chun Ke⁴

¹ Laboratory of Environmental Toxicology, National Institute of Chemical Physics and Biophysics, Akadeemia tee 23, Tallinn 12618, Estonia

² Department of Chemical and Materials Technology, Tallinn University of Technology, Ehitajate tee 5, Tallinn 19086, Estonia

³ Structure, Dynamics, and Function of Biomolecules and Molecular Complexes Laboratory, Clemson University, Clemson, SC 29634, USA

⁴ Nano-Biophysics and Soft Matter Laboratory, COMSET, Clemson University, Clemson, SC 29634, USA

⁵ Microsystems Technology and Science Laboratory, University of Michigan, Ann Arbor, MI 48109, USA

E-mail: anne.kahru@kbfi.ee and pckel1@clemson.edu


Received 2 April 2013, in final form 7 July 2013

Published 30 July 2013

Online at stacks.iop.org/Nano/24/345101

Abstract

We report on the dose-dependent inhibition of firefly luciferase activity induced by exposure of the enzyme to 20 nm citrate-coated silver nanoparticles (AgNPs). The inhibition mechanism was examined by characterizing the physicochemical properties and biophysical interactions of the enzyme and the AgNPs. Consistently, binding of the enzyme induced an increase in zeta potential from -22 to 6 mV for the AgNPs, triggered a red-shift of 44 nm in the absorbance peak of the AgNPs, and rendered a ‘protein corona’ of 20 nm in thickness on the nanoparticle surfaces. However, the secondary structures of the enzyme were only marginally affected upon formation of the protein corona, as verified by circular dichroism spectroscopy measurement and multiscale discrete molecular dynamics simulations. Rather, inductively coupled plasma mass spectrometry measurement revealed a significant ion release from the AgNPs. The released silver ions could readily react with the cysteine residues and N-groups of the enzyme to alter the physicochemical environment of their neighboring catalytic site and subsequently impair the enzymatic activity.

 Online supplementary data available from stacks.iop.org/Nano/24/345101/mmedia

(Some figures may appear in colour only in the online journal)

1. Introduction

The recent advancement of nanotechnology has transformed the landscape of modern science and engineering and, concomitantly, presented many challenges to our understanding of the biological and environmental implications of engineered nanomaterials [1, 2]. From the perspectives of biophysics and physical chemistry the interactions between

nanoparticles and biomolecules involve a description of energy minimization for the thermodynamic system, as well as characterizations of the time evolution and transformation of nanoparticle–biomolecular ‘coronas’ in changing environments (pH, temperature, salinity, and biomolecular diversity of different origin, abundance, and amphiphilicity) [3–5]. Microscopically and macroscopically such biophysical and biochemical interactions present themselves through the

endpoints of immune responses and toxicological effects on cellular and whole organism levels, yet the strategies employed by the latter fields remain to be fully validated for nanoscale objects that possess a high surface energy and reactivity as well as distinct physicochemical properties that are unavailable to bulk materials [6, 7]. Indeed, a number of studies in the recent past by our lab [8–11] and by others [3, 5, 12–15] have demonstrated the effectiveness and insight of applying the principles and methodologies of physical sciences in addressing the fate of nanoparticles in living systems. Especially on the molecular level these physical studies offer essential information complementary to the results from biological and toxicological approaches. The current study continues such an effort by examining the physicochemical and biophysical phenomena of silver nanoparticles (AgNPs) interacting with firefly luciferase and the manifestation of such interactions in the hindered activity of the enzyme.

Silver nanoparticles are a class of the most produced nanomaterials that have found their major use in antibacterial applications, in addition to their more traditional roles in catalysis and generation of surface plasmon resonance (SPR) for sensing and DNA hybridization [16–20]. The working hypotheses of the antibacterial properties of AgNPs—still much an ongoing debate today—involve the release of silver ions in the extracellular space followed by cell uptake and a cascade of intracellular reactions, direct interactions of AgNPs with cell membranes to compromise the major aspects from protein function to proton gradient and membrane permeability, and cell uptake of AgNPs which triggers the production of reactive oxygen species (ROS) and the intracellular release of silver ions to hinder DNA replication and ATP synthesis [21–24].

Information on the potentially adverse effects of AgNPs on environmentally relevant organisms is emerging [25]. With regard to the effects of AgNPs on enzymatic activities it is generally recognized that the antimicrobial action of AgNPs (and silver ions) proceeds via the inhibition of vital enzymes such as those involved in ATP production, apparently through interactions with the thiol groups of these proteins [26]. For example, Li *et al* reported that the activity of respiratory chain dehydrogenases in *Escherichia coli* was inhibited by AgNPs in a dose-dependent manner [27]. Also, soil exoenzyme activities, especially for urease and dehydrogenases, were influenced by citrate-coated AgNPs [28]. AgNPs also hindered the activity of creatine kinase from rat brain and skeletal muscle *in vitro*, presumably through interactions with the thiol groups of the enzyme [29]. It should be pointed out that ligands and enzymes with thiol groups within mammalian cells like glutathione, thioredoxin, superoxide dismutase, and thioredoxin peroxidase are key components of the cell's antioxidant defense mechanism, which is responsible for neutralizing intracellular ROS largely generated by mitochondrial energy metabolism [30].

Firefly (*Photinus pyralis*) luciferase is a 62 kDa (550 residues) protein that catalyzes the production of light by converting chemical energy into photoenergy. Specifically, this process involves the oxidation of luciferin—the heterocyclic substrate of the enzyme, in the presence of

Mg-ATP and molecular oxygen [31]. This reaction has an unusual kinetics in that luciferase turns over very slowly; after an initial flash of light, the luminescence rapidly decreases to a low level of emission, probably due to product inhibition of the enzyme.

Although the adverse effects of nanomaterials may occur on several levels for biological organizations, enzymes regulate life processes in all cells and are expected to play a pivotal role in evoking biological responses to nanomaterial exposure. In consideration of the mass production of AgNPs and also given the wide use of firefly luciferase as a reporter in a variety of *in vitro* bioassays, AgNPs and firefly luciferase were selected as a model system for our current evaluation of the biological and ecological impact of engineered nanomaterials.

In this study we examine the binding of luciferase with AgNPs and analyze the hindered enzyme activity as a result of the interaction. Specifically, using UV–vis spectrophotometry we characterize the spectral shift of the characteristic SPR of AgNPs induced by their surface coating of the (dielectric) enzyme (sections 2.3 and 3.2). We confirm the formation of an AgNP–luciferase ‘corona’ [32] using transmission electron microscopy (TEM) (sections 2.4 and 3.2) and illustrate the molecular details of such a process by state-of-the-art multiscale discrete molecular dynamics (DMD) computer simulations [33] (sections 2.8, 3.2, and 3.4). In addition, we analyze changes in the secondary structures of luciferase induced by AgNPs using circular dichroism (CD) spectroscopy (sections 2.5 and 3.2) and corroborate our observations by the simulations (sections 2.8, 3.2, and 3.4). We further characterize silver ion release from AgNPs using inductively coupled plasma mass spectrometry (ICP-MS) (sections 2.6 and 3.2) and attribute hindered enzyme luminescence to the high affinity of silver ions for the sulfhydryl (–SH) groups in the cysteine residues of the luciferase (sections 2.3, 2.7, 3.3, and 3.4). This mechanistic study offers a biophysical and physicochemical basis for facilitating our interpretation of the biological and environmental implications of nanomaterials at the molecular level.

2. Materials and methods

2.1. Materials

Citrate-coated AgNP stock suspensions (Biopure, 20 nm in diameter, 1 mg ml^{−1} in 2 mM citrate, or 0.03 × 10^{−4} M) were purchased from NanoComposix and stored at 4 °C. Citrate is widely used as a capping agent in AgNP synthesis, where the negatively charged, noncovalent citrate coating renders AgNP suspensions stable as a result of electrostatic repulsion. TRIS-acetate buffer of 25 mM, pH 7.8 was used as the test medium. TRIS base, acetic acid, and NaCl (≥99.5% purity) were purchased from J T Baker. The TRIS base was dissolved in Milli-Q water (Nanopure Diamond, Barnstead) and its pH was adjusted to 7.8 with acetic acid. QuantiLum Recombinant Firefly Luciferase (MW 62 000 Da, 13.75 mg ml^{−1} or 2.25 × 10^{−4} M) and the Luciferase Assay System were purchased

from Promega and stored at -80°C and -18°C , respectively. Silver nitrate AgNO_3 ($\geq 99.0\%$ purity), gold (III) chloride AuCl_3 ($\geq 99.99\%$ purity), and D-luciferin were purchased from Sigma Aldrich. The AgNO_3 and AuCl_3 stock solutions (1 mg ml^{-1}) were prepared in Milli-Q water and stored at 4°C . The D-luciferin stock solution (1 mg ml^{-1}) was prepared in the TRIS-acetate buffer and stored at 4°C . All experiments were performed at room temperature (20°C).

2.2. Hydrodynamic size and zeta potential

The average hydrodynamic sizes of luciferase (137.5 mg l^{-1}), AgNPs (10 mg l^{-1}), and AgNP-luciferase mixtures were determined using dynamic light scattering (DLS) (Zetasizer Nano S90, Malvern Instruments). The measurements were carried out in standard polypropylene plastic cuvettes of 1 cm path length. The surface charges of the samples were measured in Milli-Q water to avoid interference of TRIS-acetate buffer on the analytes' potentials, using a Zetasizer Nano ZS (Malvern instruments). Different luciferase concentrations were titrated with the AgNP suspensions. The samples were allowed to stabilize for 2 h at room temperature prior to the zeta potential measurement.

2.3. UV-vis spectrophotometry

The binding of luciferase (13.75 mg l^{-1}) to AgNPs (10 mg l^{-1}) was investigated by measuring the SPR peak (350–500 nm wavelength) of the AgNPs using a UV-vis spectrophotometer (Cary 300 Bio, Varian). This measurement was done in Milli-Q water at room temperature using a polypropylene plastic cuvette of 1 cm path length. The binding affinities of luciferase (200 mg l^{-1}), ATP (100 mg l^{-1}), and luciferin (50 mg l^{-1}) for silver ions were investigated using the UV-vis spectrophotometer and quartz cuvettes of 1 cm path length.

2.4. TEM

Direct observation of AgNP-luciferase coronas was performed by TEM (Hitachi H7600). Specifically, AgNPs (1 mg l^{-1}) were incubated with luciferase (13.75 mg l^{-1}) for 2 h, pipetted on a copper grid, and stained with phosphotungstic acid for 10 min prior to imaging. The same procedure was applied to control samples of AgNPs (1 mg l^{-1}) alone. All dilutions were performed in 25 mM TRIS-acetate buffer and stored at room temperature.

2.5. CD spectroscopy

A spectrometer (J-810, Jasco) was used to assess the effects of AgNP binding on the secondary structures of the enzyme. For this purpose, luciferase (13.75 mg l^{-1}) was incubated with AgNPs (1 mg l^{-1}) and silver ions (1 mg l^{-1}) for 2 h at room temperature and the measurement was performed in a quartz cuvette of 1 cm path length between 190 and 300 nm at 1 nm intervals. The selection of this wavelength range

avoided strong absorption and SPR from the AgNPs. The backgrounds of the AgNPs and the silver ions were subtracted accordingly to exclude their interferences with that of the luciferase. Milli-Q water instead of the TRIS buffer was used to minimize interference to the CD signal from the buffer.

2.6. ICP-MS

Silver ion release from citrate-coated AgNPs, upon their incubation with luciferase, was performed using ICP-MS (X Series 2, Thermo Scientific). For this measurement AgNPs (1 mg l^{-1}) and luciferase (13.75 mg l^{-1}) were mixed in TRIS-acetate buffer and incubated at room temperature for 0, 2, 4, 8, 24, 48, and 72 h in polypropylene Eppendorf tubes. At each time point the samples were centrifuged at 12 100 RCF (MiniSpin, Eppendorf) for 30 min, and the supernatants were collected and stored at -18°C . The effectiveness of centrifugation for the precipitation of AgNPs was confirmed by measuring UV-vis absorbance for the suspensions before and after the procedure. The effect of luciferase concentration (2.74, 6.85, 13.75, 137.5 mg l^{-1}) on ion release from the AgNPs (1 mg l^{-1}) was determined using the procedure described above, for 24 h incubation. Prior to the ICP-MS analysis the samples were thawed and diluted 10-fold in 2% HNO_3 .

2.7. Luciferase activity assay

The effect of AgNPs on luciferase activity was determined using the Luciferase Assay System (Promega). The assay was first calibrated for the concentrations of luciferase (10^{-8} – 10^{-17} M) and the AgNPs (0.01, 0.1, 1, 10, 100 mg l^{-1}). For the study of the inhibitory effect of silver ions, AgNO_3 of 0.002, 0.02, 0.2, 2, and 20 mg l^{-1} was used and the testing was conducted following the same procedures as for the AgNPs. The concentrations of silver ions were chosen by taking into account that AgNPs released $\sim 20\%$ of their mass to silver ions in 2 h. Luciferase was incubated with AgNPs or AgNO_3 for 2 h at room temperature prior to the measurement. A pre-incubated AgNP-luciferase mixture of $20\text{ }\mu\text{l}$ was added to $100\text{ }\mu\text{l}$ of the Luciferase Assay System and the signal was recorded with a luminometer (Turner BioSystem 20/20n). The luciferase activity assay was also performed in the presence of Na^+ (as NaCl ; 2, 20, 200 mg l^{-1} of Na l^{-1}) or Au^{3+} (as AuCl_3 ; 0.002– 200 mg Au l^{-1}) to determine the specificity of the observed inhibition. In order to identify if any of the reaction components in the Luciferase Assay System limited luciferase activity, a kinetic study was performed where an extra $20\text{ }\mu\text{l}$ of luciferase, ATP (100 mg l^{-1}), or luciferin (100 mg l^{-1}) was added to the assay after 20 min of reaction and the resulting luminescence was recorded for the next 20 min.

In addition, a rapid kinetics assay was performed for the luminescence reaction (Orion II luminometer, Berthold Technologies). This experiment was conducted at room temperature using 96-well white polypropylene microplates. A Luciferase Assay System reagent of $100\text{ }\mu\text{l}$ and nanoparticle suspensions or ions of $10\text{ }\mu\text{l}$ (0.4 – 400 mg Ag l^{-1}) were

Table 1. Zeta potentials of luciferase–AgNP mixtures at different enzyme concentrations. Prior to the measurements AgNPs of 10 mg l⁻¹ were pre-incubated with luciferase of different concentrations for 2 h in Milli-Q water. Data presented are the averages of three samples ± standard deviations.

Sample	Zeta potential (mV)
137.5 mg l ⁻¹ luciferase	3.2 ± 0.2
137.5 mg l ⁻¹ luciferase + 10 mg l ⁻¹ AgNPs	6.0 ± 0.3
13.8 mg l ⁻¹ luciferase + 10 mg l ⁻¹ AgNPs	4.5 ± 0.5
6.8 mg l ⁻¹ luciferase + 10 mg l ⁻¹ AgNPs	-5.0 ± 0.8
2.8 mg l ⁻¹ luciferase + 10 mg l ⁻¹ AgNPs	-19.3 ± 0.3
10 mg l ⁻¹ AgNPs	-22.0 ± 0.3

pipetted into each well. Then luciferase of 20 μl was automatically dispensed into the microplate wells in the luminometer testing chamber. The luminescence was recorded during the first 10 s at 5 data points s⁻¹.

2.8. Computer simulation of AgNP–luciferase binding

Multiscale DMD simulations [33] were applied to study the interactions between luciferase and AgNPs *in silico*. Specifically, atomistic simulations [34] were used to identify the binding modes between an individual luciferase and a citrate-coated AgNP, and coarse-grained simulations [35] were used to characterize the corona formation between multiple luciferase molecules and one citrate-coated AgNP. DMD is a special type of molecular dynamics simulation algorithm [36], which features high sampling efficiency and has been increasingly used to study biomolecules [37]. A model citrate-coated AgNP of 10 nm in diameter as detailed recently [38] was employed for the current study, where the surface silver atoms of the nanoparticle were mostly hydrophobic without charges and only a small fraction of the surface atoms were positively charged. This approach of using a smaller AgNP in the simulations than in the experiments (20 nm in diameter) significantly reduced the computational cost without compromising much of the physical phenomena under examination. The x-ray crystallography structure of the luciferase from *Photinus pyralis* was used as a reference structure (PDB [39] ID: 1BA3).

3. Results and discussion

3.1. An empirically determined luciferase to AgNP ratio

The mean diameter of AgNPs was 20 ± 3 nm as specified by the manufacturer, and the QuantiLum Recombinant Firefly Luciferase (MW 62 000 Da) was ~6 nm in size. Based on the surface areas and sizes of the AgNPs and the luciferase, the optimized enzyme to nanoparticle ratio of N was calculated as follows:

$$N = \frac{4\pi(R_{\text{Ag}} + R_{\text{Luciferase}})^2}{\pi R_{\text{Luciferase}}^2}, \quad (1)$$

where R_{Ag} and $R_{\text{Luciferase}}$ are the radii of AgNPs and luciferase, respectively. According to this equation, it is estimated that up to 75 luciferase molecules can be adsorbed onto each individual AgNP, equivalent to a concentration ratio of 137.5 mg l⁻¹ of luciferase to 10 mg l⁻¹ of AgNPs.

3.2. Physicochemical interactions of luciferase and AgNPs

The hydrodynamic size of AgNPs in 25 mM TRIS-acetate buffer (pH 7.8) was measured to be 26.2 ± 0.1 nm, consistent with the specifications provided by the manufacturer. However, luciferase displayed significant agglomerations in the test medium (>1 μm), making it difficult to infer the hydrodynamic size of AgNPs upon luciferase adsorption. Nonetheless, binding of the enzyme to AgNPs was evidenced from the zeta potential measurement through titrating different concentrations of luciferase into the AgNP suspensions (10 mg l⁻¹). As shown in table 1 the AgNPs exhibited a negative surface charge (-22 mV) in Milli-Q water due to their citrate coating. Under the same conditions luciferase alone showed a slightly positive surface charge (3.2 mV) as a net result from its positively and negatively charged domains. With increasing concentrations of luciferase the mixtures of luciferase–AgNPs displayed a steady increase in zeta potential up to 6 mV, suggesting binding of the enzyme and the nanoparticles (and their citrate coating), driven by *van der Waals* forces, electrostatic interactions, dynamic exchanges between the enzyme and citrate for their adsorption onto the nanoparticle surfaces, as well as hydrogen bonding between the citrate and the electronegative moieties of the protein.

The formation of AgNP–luciferase corona was confirmed by a comparison of the UV–vis spectra of AgNPs, luciferase, and their mixture (figure 1(a)). The AgNP–luciferase mixture was stable at 2 h, but showed a 24.7% reduction in absorbance at 20 h due to precipitations over time. A characteristic peak of SPR was identified for AgNPs at 402 nm (blue curve). A red-shift of 44 nm in the extinction peak of AgNPs occurred after their incubation with luciferase, accompanied by a decrease of 14% in the magnitude of the peak value. This phenomenon is consistent with our previous study on the binding of AgNPs with human serum albumin [40], indicating an increased dielectric constant for the AgNPs as a result of protein adsorption/coating and nanoparticle aggregation.

The inset of figure 1(b) shows a TEM micrograph of the control AgNPs, which were well dispersed and were approximately spherical. The size of the AgNPs ranged between 21.4 and 24.8 nm, consistent with the manufacturer's information and our DLS measurement. In the presence of luciferase, a thick layer of optically less dense material was clearly visible surrounding the AgNPs (figure 1(b)). The average diameter of the AgNP–luciferase coronas was

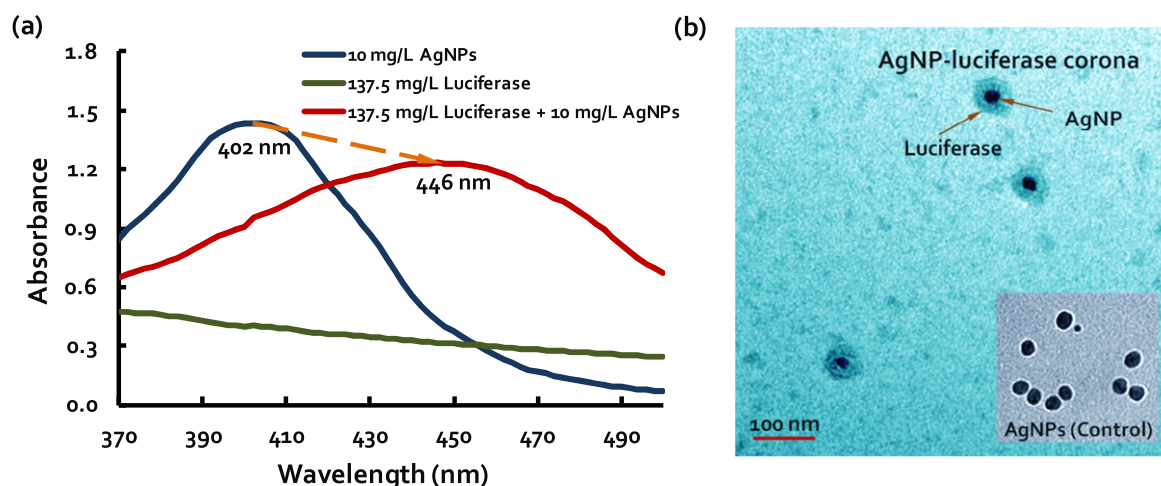


Figure 1. Interactions of AgNPs with luciferase. (a) UV-vis spectra and (b) TEM image. The maroon line in panel (a) describes a spectrum of the AgNP-luciferase mixture and displays a red-shift of 44 nm and a 14% decrease in absorbance value for the SPR peak of AgNPs (blue) as a result of luciferase binding and nanoparticle aggregation. The green line indicates the absorbance of the enzyme. The TEM image (b) shows AgNP-luciferase coronas. Inset in (b): control AgNPs. Scale bar: 100 nm for both the image and the inset.

determined to be ~ 60 nm and the average thickness of the protein layers was ~ 20 nm. This image corroborates the binding of the enzyme with the AgNPs and implies multilayer protein coating of the nanoparticles.

CD spectroscopy was performed to determine the effect of AgNP and silver ion binding on the secondary structures of the luciferase. Our measurement (figure S1 available at stacks.iop.org/Nano/24/345101/mmedia) revealed a decrease of beta sheets from 26% to 22% (or a relative decrease of 15.4%) and a corresponding increase of alpha helices from 20% to 22% (or a relative increase of 10%) after incubating the protein ($500\times$ dilution from stock, i.e., 27.5 mg l^{-1}) with the AgNPs (0.9 mg l^{-1}) in Milli-Q water. Due to the differences in their surface curvatures, the globular luciferase molecules (~ 6 nm) could sense the AgNPs (~ 20 nm) as relatively flat substrates upon their binding. In addition, since the enzyme formed a multilayer coating the protein conformation of the outer layers could be affected by the inner layers without direct contact with the particle surfaces. Consequently, modest conformational changes were induced and the enzyme was later shown in the activity assay and in the computer simulations as only slightly perturbed by the physical adsorption of the nanoparticles. Similar to the trend observed for proteins exposed to AgNPs, silver ions in AgNP suspensions could also alter the protein conformation, as indicated by the CD measurement on luciferase incubated with free silver ions (figure S1, blue line, where beta sheets decreased from 26% to 23% and alpha helices increased from 20% to 21% as derived from the spectrum).

AgNPs released silver ions upon their incubation with the enzyme in aqueous solutions. The released silver ions have been evidenced to be highly reactive to inhibit respiratory enzymes, induce overproduction of ROS, and bind sulfur- and phosphorus-containing molecules to interrupt cell defense systems or deplete intracellular concentrations of such molecules [30]. Indeed, our data showed that AgNPs (1 mg l^{-1}) were completely dissolved during 24 h in the

test medium. In the presence of luciferase our ICP-MS measurement revealed a significantly reduced ion release from the AgNPs over time (figure 2(a)), conceivably due to the blockage by the adsorbed proteins. Specifically, the mixture of luciferase (137.5 mg l^{-1}) and AgNPs (1 mg l^{-1}) showed 15% dissolution of the AgNPs after 4 h and the ion release was terminated after 72 h. For a given AgNP concentration (1 mg l^{-1}) and at 24 h of incubation, when the luciferase concentration was reduced from 137.5 to 2.74 mg l^{-1} the silver ion release was increased from 7 to 641 μ g of Ag^+ l^{-1} (figure 2(b)).

3.3. Luciferase enzymatic activity

A luciferase concentration of 10^{-9} M in the middle of the calibrated linear response curve (data not shown) was chosen for examining the enzymatic activity. Our experiment showed that AgNPs inhibited light producing a reaction catalyzed by the luciferase, mirroring the same tendency found for the reaction with Ag^+ alone (figure 3). The luminescence signals were comparable for AgNPs and Ag^+ of concentrations equivalent to $\sim 20\%$ of the AgNPs in mass, in agreement with the 2 h ion release from AgNPs determined by the ICP-MS experiment (figure 2(a)). This assay suggests that the inhibition of luciferase was largely induced by silver ions while the physical adsorption onto AgNPs and its induced crowding and conformational changes in protein structure only exerted a minor effect on the enzyme function. The latter point was further corroborated by the DMD simulation described in section 3.4.

Additional UV-vis absorbance measurements were conducted to investigate the binding affinities of silver ions for the reaction components ATP, luciferase, and luciferin (figure S2 available at stacks.iop.org/Nano/24/345101/mmedia). Overall Ag^+ showed a higher affinity for luciferase than for ATP or luciferin, judged by the corresponding spectral changes for these ligands. This

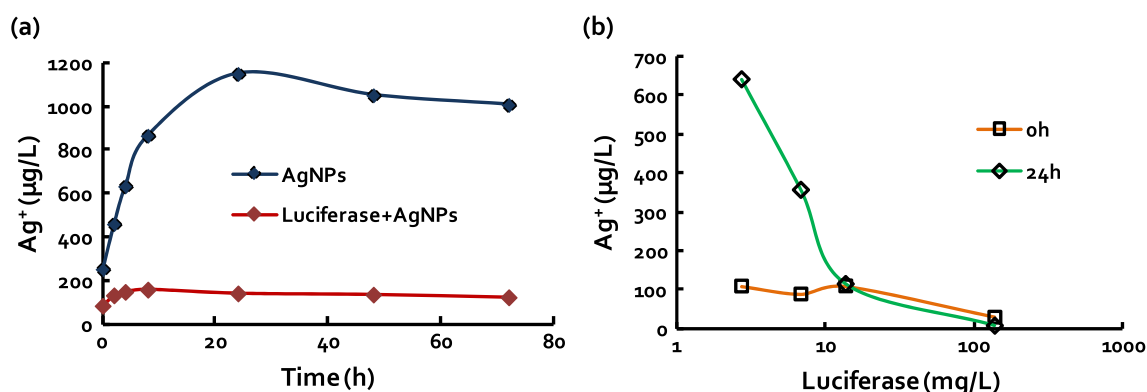


Figure 2. Effects of incubation and luciferase concentration on silver ion release from AgNPs. (a) 1 mg l^{-1} of AgNP suspension was incubated with and without luciferase (137.5 mg l^{-1}) for 72 h. (b) 1 mg l^{-1} of AgNP suspension was incubated with luciferase of $2.64\text{--}137.5 \text{ mg l}^{-1}$. The concentrations of silver ions are shown for two time points (0 and 24 h). The ion release experiment was performed first by sample centrifugation and supernatant collection. The quality of the samples was controlled by UV-vis and DLS to ensure the absence of nanoparticles after centrifugation. The ICP-MS measurement was then performed with three parallels. The samples had $\sim 20\%$ ions at the 'zero point' of measurement immediately after dilutions and centrifugations.

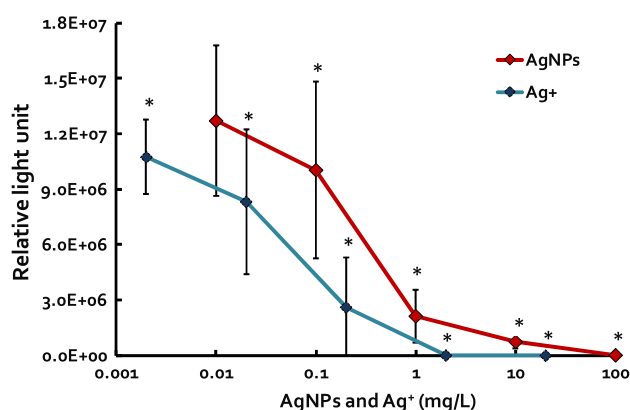


Figure 3. Inhibition of luciferase activity by AgNPs and Ag^+ . Statistically significant differences between the samples and the controls (i.e., when neither AgNPs nor silver ions were applied to the reaction) were determined by the Student *t*-test (asterisk * indicates $p < 0.05$). This experiment was performed using three independent replicates and the average values are presented.

measurement further suggests that the limiting factor in the inhibition of luciferase luminescence was the interaction between the enzyme and silver ions. Consistently, our kinetic study showed a recovery of luminescence intensity upon addition of extra luciferase 1200 s into the reaction (figure 4(a)), while no such recovery was observed for the addition of extra ATP or luciferin (data not shown). Since our assay with Au^{3+} (figure 4(c)) showed a similar but less pronounced inhibition pattern than that observed for Ag^+ , unlike the case with Na^+ (figure 4(b)), we further attribute the observed luminescence inhibition to the interactions of Ag^+ or Au^{3+} with the sulfhydryl groups in the cysteine residues of the luciferase. The strengths of such thiol-heavy metal bonds are of the order of 100 kJ mol^{-1} and are often utilized to render molecular self-assemblies that are stable in a variety of temperatures, solvents, and potentials [41]. *N*-containing functional groups could also complex with

Ag^+ or Au^{3+} . However, the strength of such complexation would be weaker than the disulfide bonds formed between Ag and cysteines. Although the covalent-like thiol-Au bond is slightly stronger than the thiol-Ag bond according to density functional theory calculations [42], the structural stability of the protein and the spatial distribution (and hence differential accessibility) of the cysteine residues (figure 5(a)) should favor their bond formation with the monovalent Ag^+ over the trivalent Au^{3+} , as reflected by a lack of rapid inhibition induced by Au^{3+} (figure S3(c) available at stacks.iop.org/Nano/24/345101/mmedia) and the differential inhibition efficiencies associated with the two types of heavy metals after 2 h of incubation (figure 4(c)). Firefly luciferase possesses four cysteine residues per monomer, all of which are positioned away from the active site (figure 5(a)) with the shortest distance $\sim 1.5 \text{ nm}$. Although it does not appear that a specific cysteine mediates the loss of luciferase activity, complete inactivation of luciferase activity has been demonstrated by the blockage of all four cysteine thiols and the concomitant incorporation of four moles of *N*-acetyl-*N'*-(5-sulfo-1-naphthyl)ethylenediamine (AEDANS) per mole of enzyme [43]. Nonetheless, such interactions between silver ions and cysteine residues ought to alter the enzyme conformation directly or allosterically, modify the local environment (charge, amphiphilicity, and accessibility) of the enzyme active site to impair its interactions with luciferin, ATP, oxygen, and cofactors and further hinder the catalysis of light emission.

3.4. DMD simulation of AgNP-luciferase corona

We first performed all-atom DMD simulations of a luciferase molecule interacting with a citrate-coated AgNP. We started with the apo-structure of luciferase (figure 5(a), left panel) initially positioned away from the AgNP. Independent simulations with different starting configurations suggested that the inter-molecular interactions were dominated by

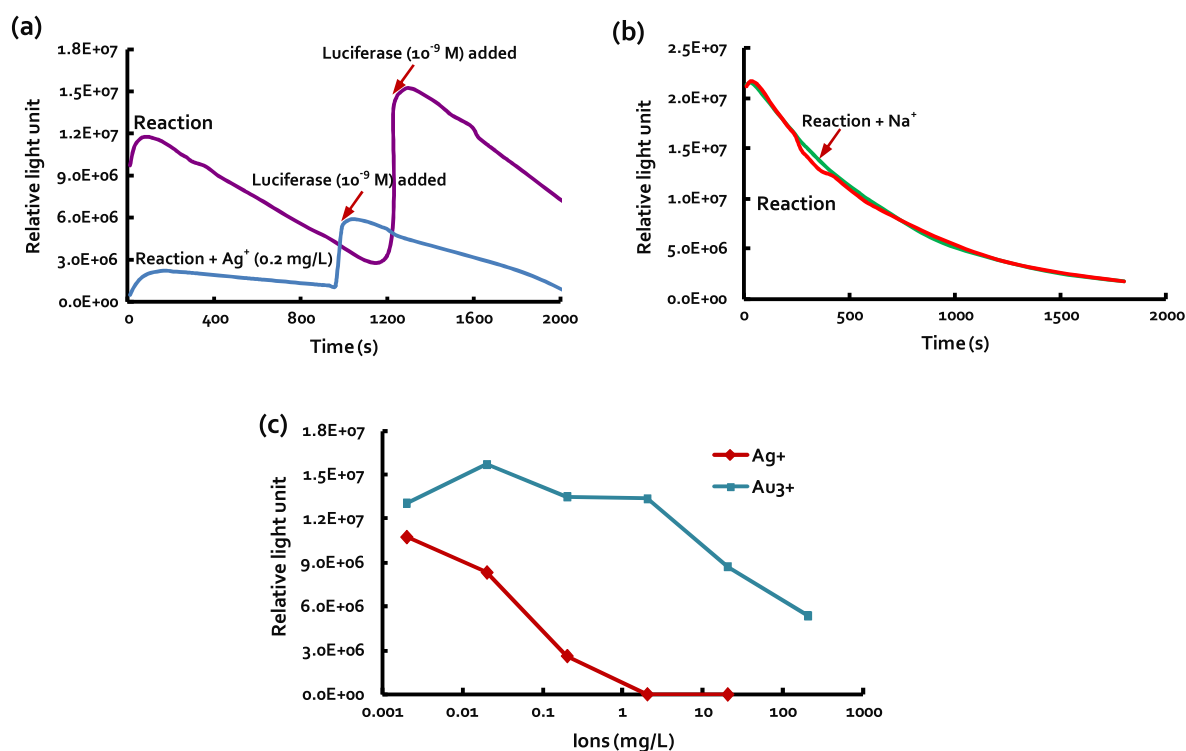


Figure 4. Inhibition of luciferase activity by silver and gold ions. (a) Luminescence kinetics upon addition of extra luciferase after 1200 s of reaction. The addition of luciferase resulted in an increase in luminescence intensity while no such effect was observed for the addition of ATP or luciferin (data not shown). (b) No effect on reaction kinetics was observed with the addition of Na^+ . (c) A comparison of the inhibitory effects of Ag^+ and Au^{3+} on enzyme activity. Each data curve was averaged over three independent measurements.

electrostatic attraction between the negatively charged luciferase residues and the positively charged domains of the AgNP surface (figure 5(b)). Interestingly, we observed that the luciferase molecule could adopt a holo-like structure with the C-terminal domain packed closely against the N-terminal domain (figure 5(b)) during the simulations, suggesting that two luciferase sub-domains (figure 5(a)) are flexible and that the holo-like structure is thermodynamically stable in the absence of a substrate. Despite the inter-domain flexibility, each of the sub-domains remained native-like upon binding to the AgNP. This observation is consistent with the CD experiment as well as the activity assay where the AgNP-bound luciferase was still active with its bioluminescent function. Although the effect of cysteine–Ag coordination was not studied in our simulations due to the lack of thiol–Ag bond parameterization in our current force field [34], these simulations have excluded the direct role of AgNPs in causing the inhibition of luciferase luminescence.

Based on the specific inter-molecular interactions extracted from multiple all-atom DMD simulations, we built a coarse-grained model of AgNP–luciferase interactions [38]. We performed the coarse-grained DMD simulation of ten luciferase molecules interacting with one citrate-coated AgNP (figure 5(c)). A protein molecule was found to either bind directly to the AgNP or interact with the proteins already bound to the nanoparticle. The direct AgNP–protein contact was a result of the interactions between the nanoparticle and a specific set of the luciferase residues (figure S4 available at stacks.iop.org/Nano/24/345101/mmedia), as determined from

the atomistic simulations. The indirect interaction was due to the non-specific protein–protein attractions (figure 5(c)), which were found important for protein aggregation and association [35]. A three-layer luciferase corona corresponds to an increase of ~ 20 nm in radius as observed in the TEM experiment (figure 1(b)). Although computationally too expensive to demonstrate, we expect that a multilayer AgNP–luciferase corona would form in the simulation with a significantly longer observation time and a higher stoichiometric ratio of proteins to nanoparticles.

4. Conclusions

In summary, we have investigated the binding of luciferase with citrate-coated AgNPs and established a crucial connection between such physical interactions and their endpoint in the hindered enzyme activity. Although luciferase readily bound to AgNPs through electrostatic interactions, *van der Waals* forces, dynamic exchanges with the citrate, as well as hydrogen bonding to render a protein corona as evidenced by our physicochemical characterizations and state-of-the-art DMD computer simulations, little conformational changes in the enzyme resulted from such direct interactions. Instead, AgNPs readily released silver ions to dose-dependently inhibit the enzymatic activity, on both short (i.e., sub-seconds to seconds) and long (i.e., minutes to hours) timescales. An analogous inhibition pattern was observed for Au^{3+} but not for Na^+ . Conceivably, silver ions were bound to the cysteine residues ~ 20 Å away from the catalytic site of the protein

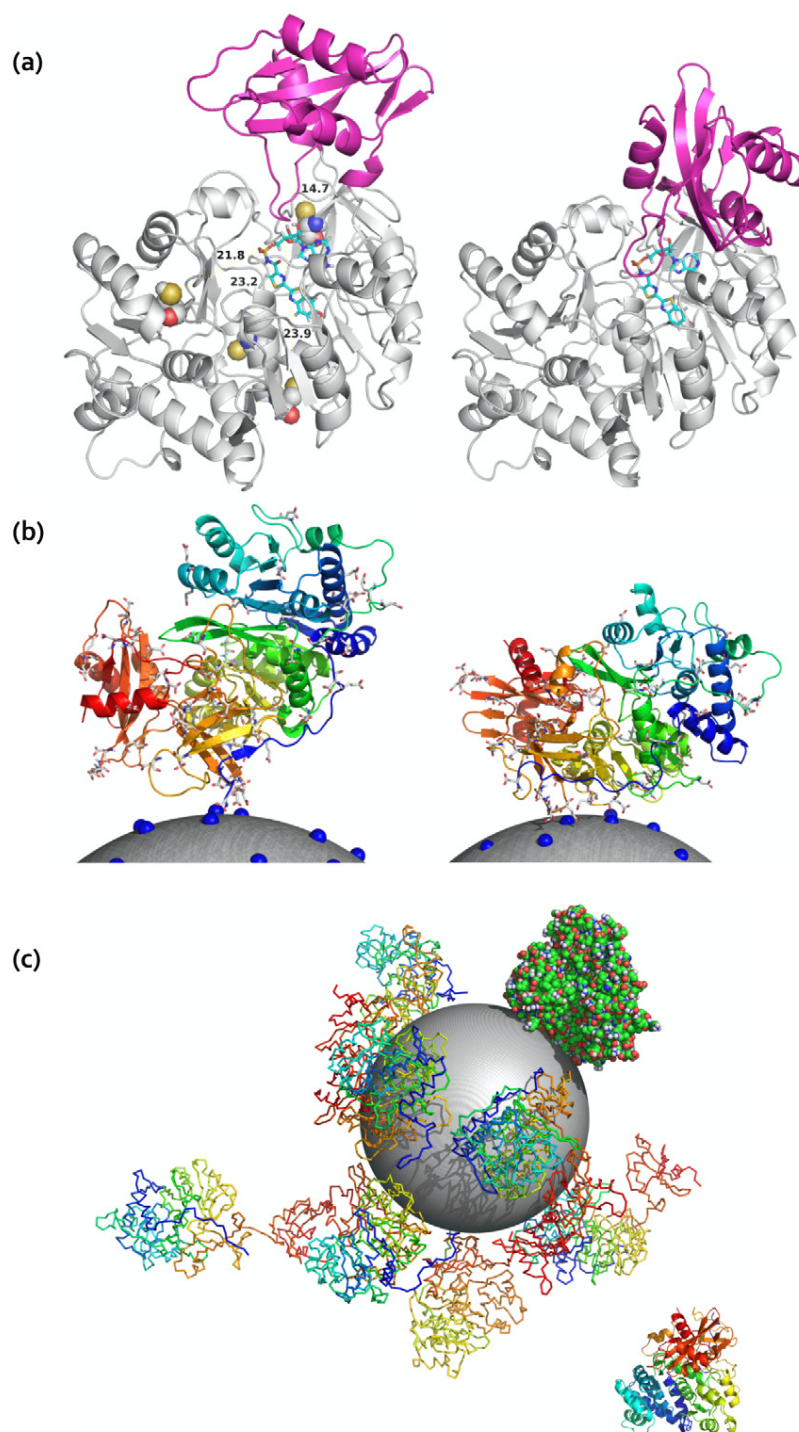


Figure 5. DMD simulation of AgNP-luciferase corona. (a) The apo- (left panel; PDB ID: 1BA3) and holo- (right panel; PDB ID: 2D1S) structure of luciferase. The C-terminal domain (in red) undergoes major conformational changes upon binding to substrates and is packed against the N-terminal domain (in gray) to form a more compact holo-conformation. The distances between the four cysteine residues (as spheres) and a substrate in the active site (as sticks in cyan color) are specified (in Å) for the apo-structure. (b) Two representative AgNP-luciferase binding conformations. The large gray sphere represents the AgNP and the blue spheres denote the surface positive charges of the nanoparticle. The protein is rainbow colored from blue (N-terminal) to red (C-terminal). The negatively charged residues are shown in sticks. (c) A typical snapshot of the coarse-grained simulation of ten luciferase proteins interacting with one AgNP. An AgNP-bound protein is shown in spheres, illustrating its contacts with the nanoparticle, and an incoming protein is illustrated in cartoon representation. The rest of the proteins are shown in backbone-trace representation.

and directly or allosterically altered the conformation and physicochemical environment of the protein to hinder its luminescence reaction. Silver ions could also complex with

the N-groups of the protein, though likely of less impact on protein conformation and function than the thiol-Ag bond. Taken together, this study offers a much needed biophysical

perspective for advancing our understanding of the biological and environmental implications of nanomaterials.

Acknowledgments

This research was supported by NSF grant no. CBET-1232724 to Ke, a graduate mobility grant to Käkinen from the Archimedes Foundation of Estonia, and EU FP7 NanoValid and ETF grant no. 8561 to Kahru and Käkinen. The authors thank Dr William Baldwin for providing the Turner BioSystem luminometer and Dr Brian Powell and Aby Thyparambil for assisting the ICP-MS and CD measurements.

References

- [1] Wiesner M, Lowry G V, Alvarez P, Dionysiou D and Biswas P 2006 *Environ. Sci. Technol.* **40** 4336
- [2] Nel A, Xia T, Madler L and Li N 2006 *Science* **311** 622
- [3] Nel A E, Mädler L, Velegol D, Xia T, Hoek E M, Somasundaran P, Klaessig F, Castranova V and Thompson M 2009 *Nature Mater.* **8** 543
- [4] Ke P C and Lamm M H 2011 *Phys. Chem. Chem. Phys.* **13** 7273
- [5] Xia X R, Monteiro-Riviere N A, Mathur S, Song X, Xiao L, Oldenberg S J, Fadeel B and Riviere J E 2011 *ACS Nano* **5** 9074
- [6] Maynard A D et al 2006 *Nature* **444** 267
- [7] Baun A, Hartmann N B, Grieger K and Kusk K O 2008 *Ecotoxicology* **17** 387
- [8] Qiao R, Roberts A P, Mount A S, Klaine S J and Ke P C 2007 *Nano Lett.* **7** 614
- [9] Salonen E, Lin S, Reid M L, Allegood M S, Wang X, Rao A M, Vattulainen I and Ke P C 2008 *Small* **4** 1986
- [10] Ratnikova T A, Govindan P N, Salonen E and Ke P C 2011 *ACS Nano* **5** 6306
- [11] Chen R, Ratnikova T A, Stone M B, Lin S, Lard M, Huang G, Hudson J S and Ke P C 2010 *Small* **6** 612
- [12] Wong-ekkabut J, Baoukina S, Triampo W, Tang I M, Tieleman D P and Monticelli L 2008 *Nature Nanotechnol.* **3** 363
- [13] Barnard A S 2009 *Nature Nanotechnol.* **4** 332
- [14] Kubiak K and Mulheran P A 2009 *J. Phys. Chem. B* **113** 12189
- [15] Hung A, Mwenifumbo S, Mager M, Kuna J J, Stellacci F, Yarovsky I and Stevens M M 2011 *J. Am. Chem. Soc.* **133** 1438
- [16] Jin X, Li M, Wang J, Marambio-Jones C, Peng F, Huang X, Damoiseaux R and Hoek E M V 2010 *Environ. Sci. Technol.* **44** 7321
- [17] Choi O and Hu Z 2008 *Environ. Sci. Technol.* **42** 4583
- [18] Kennedy A, Hull M, Bednar A J, Goss J, Gunter J, Bouldin J, Vikesland P and Steevens J 2010 *Environ. Sci. Technol.* **44** 9571
- [19] Fabrega J, Renshaw J C and Lead J R 2009 *Environ. Sci. Technol.* **43** 9004
- [20] Croteau M-N, Misra S K, Luoma S N and Valsami-Jones E 2011 *Environ. Sci. Technol.* **45** 6600
- [21] Zhang W, Yao Y, Sullivan N and Chen Y 2011 *Environ. Sci. Technol.* **45** 4422
- [22] Sotiriou G A and Pratsinis S E 2010 *Environ. Sci. Technol.* **44** 5649
- [23] Kittler S, Greulich C, Diendorf J, Koller M and Epple M 2010 *Chem. Mater.* **22** 4548
- [24] Navarro E, Piccapietra F, Wagner B, Marconi F, Kaegi R, Odzak N, Sigg L and Behra R 2008 *Environ. Sci. Technol.* **42** 8959
- [25] Kahru A and Dubourguier H C 2010 *Toxicology* **269** 105
- [26] Louie A Y and Meade T J 1999 *Chem. Rev.* **99** 2711
- [27] Li W R, Xie X B, Shi Q S, Zeng H Y, Ou-Yang Y S and Chen Y B 2010 *Appl. Microbiol. Biotechnol.* **85** 1115
- [28] Shin Y J, Kwak J I and An Y J 2012 *Chemosphere* **88** 524
- [29] Paula M M S, Costa C S, Baldin M C, Scaini G, Rezin G T, Segala K, Andrade V M, Franco C V and Streck E L 2009 *J. Braz. Chem. Soc.* **20** 1556
- [30] Chen X and Schluesener H J 2008 *Toxicol. Lett.* **176** 1
- [31] Conti E, Franks N P and Brick P 1996 *Structure* **4** 287
- [32] Cedervall T, Lynch I, Lindman S, Berggard T, Thulin E, Nilsson H, Dawson K A and Linse S 2007 *Proc. Natl Acad. Sci. USA* **104** 2050
- [33] Ding F, Furukawa Y, Nukina N and Dokholyan N V 2012 *J. Mol. Biol.* **421** 548
- [34] Ding F, Tsao D, Nie H and Dokholyan N V 2008 *Structure* **16** 1010
- [35] Ding F, Dokholyan N V, Buldyrev S V, Stanley H E and Shakhnovich E I 2002 *J. Mol. Biol.* **324** 851
- [36] Rapaport D C 1997 *The Art of Molecular Dynamics Simulation* (Cambridge: Cambridge University Press)
- [37] Ding F and Dokholyan N V 2012 Discrete molecular dynamics simulation of biomolecules *Computational Modeling of Biological Systems: From Molecules to Pathways* ed N V Dokholyan (Berlin: Springer) pp 57–74
- [38] Ding F, Radic S, Chen R, Chen P, Geitner N K, Brown J M and Ke P C 2013 Direct observation of a silver nanoparticle-ubiquitin corona formation *Nanoscale* **at press**
- [39] Berman H M, Westbrook J, Feng Z, Gilliland G, Bhat T N, Weissig H, Shindyalov I N and Bourne P E 2000 *Nucl. Acids Res.* **28** 235
- [40] Chen R, Choudhary P, Schurr R N, Bhattacharya P, Brown J M and Ke P C 2012 *Appl. Phys. Lett.* **100** 013703
- [41] Weisbecker C S, Merritt M V and Whitesides G M 1996 *Langmuir* **12** 3763
- [42] Kacprzak K A, Lopez-Acevedo O, Hakkinen H and Gronbeck H 2010 *J. Phys. Chem. C* **114** 13571
- [43] Branchini B R, Magyar R A, Murtiashaw M H, Magnasco N, Hinz L K and Stroh J G 1997 *Arch. Biochem. Biophys.* **340** 52